AD-A168 876 ON THE SAMPLING EFFICIENCY OF A LARGE DOWNWARD INLET AEROSOL SAMPLER(U) DEFENCE RESEARCH ESTABLISHMENT VALCARTIER (QUEBEC) G ROY MAY 86 DREV-4399/86 1/1

UNCLASSIFIED F/G 20/4 NL

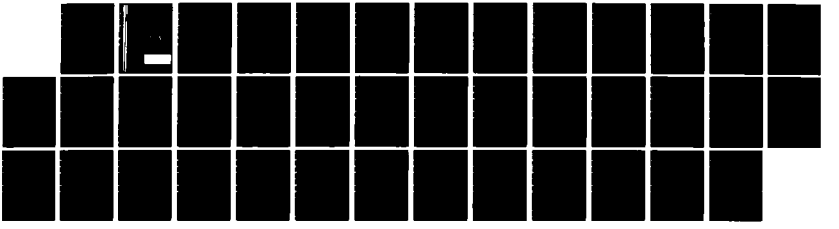

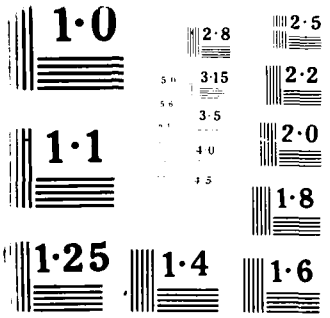
1·0
2·8
2·5
3·15
2·2
3·5
1·1
2·0
4·0
4·5
1·8
1·25
1·4
1·6

National Defence
Defence nationale

UNCLASSIFIED
UNLIMITED DISTRIBUTION

(3)

DREV REPORT 4399/86
FILE 3621B-005
MAY 1986

CRDV RAPPORT 4399/86
DOSSIER 3621B-005
MAI 1986

ON THE SAMPLING EFFICIENCY OF A LARGE DOWNWARD INLET AEROSOL SAMPLER

G. Roy

Defence Research Establishment
Centre de recherches pour la Défense,
Valcartier, Québec

Canada

SANS CLASSIFICATION
DISTRIBUTION ILLIMITÉE

DREV R-4399/86
FILE: 3621B-005

UNCLASSIFIED

CRDV R-4399/86
DOSSIER: 3621B-005

ON THE SAMPLING EFFICIENCY OF A LARGE DOWNWARD INLET AEROSOL SAMPLER

by

G. Roy

DEFENCE RESEARCH ESTABLISHMENT

CENTRE DE RECHERCHES POUR LA DÉFENSE

VALCARTIER

Tel: (418) 844-4271

Québec, Canada

May/mai 1986

SANS CLASSIFICATION

ABSTRACT

A computer simulation has been used to calculate the sampling efficiency of a downward-facing aerosol sampler having a large entrance aperture. Flow-field calculations have been done by solving the Laplace equation for a flat disk with uniform air velocity over its surface. Initial positions from which particles reach an equilibrium position at which the sedimentation speed equals the air suction speed of the sampler are obtained by iterative solution of the equations of motion. These distances are time-independent and are called critical distances. The time-dependent sampling efficiency is obtained by combining critical distances with the sampler interaction distance for a given sample volume of air. The effect on sampling efficiency of various parameters such as the sampling flow rate, sampling period, height of the aerosol above the filter, and rim size is evaluated.

RÉSUMÉ

Une simulation sur ordinateur a été utilisée pour calculer l'efficacité d'un échantillonneur d'aérosol inversé à grande ouverture. Les champs d'écoulement ont été calculés en solutionnant l'équation de Laplace pour un disque plat dont la vitesse de l'air est uniforme sur la surface. Les positions initiales desquelles les particules aboutissent en équilibre à une position où la vitesse de sédimentation égale la vitesse de succion de l'air de l'échantillonneur sont établies par itération des équations du mouvement. Ces distances, appelées distances critiques, sont indépendantes du temps. La dépendance temporelle de l'efficacité d'échantillonnage est obtenue en combinant les distances critiques et la distance d'interaction pour un certain volume d'air. L'influence sur l'efficacité d'échantillonnage des paramètres tels que le débit et la période d'échantillonnage, la hauteur d'aérosol au-dessus de l'échantillonneur et la largeur du rebord est calculée.

TABLE OF CONTENTS

NOMENCLATURE

a	sampler aperture
A	semi-minor axis along R (representation of a potential line by an ellipse)
AC	semi-major axis along R (representation of critical position AS by an ellipse)
$\overline{AC}$	mean interactive distance during the sampling period T
AS	critical position along R for a given Z_1 and s
B	semi-major axis along Z (representation of a potential line by an ellipse)
BC	semi-minor axis along Z (representation of critical position AS by an ellipse)
E	sampling efficiency
g	gravitation constant 981 cm/s^2
h	height of aerosol above the sampler
H (s,T)	function related to the height of the aerosol above the sampler
J_1	Bessel function of order 1
L	sampler radius
Q	sampling flow rate
r	particle radius
R	particle coordinate along R-axis
R_1	initial particle coordinate along R-axis
s	ρr^2 - defines particle mass size
S (s,T)	function related to the surface crossed by particles under sedimentation and to the sampled volume of air
T	sampling period

$T_{AC}(s_2)$	time required for the air at position $AC(s_2)$ to reach the filter paper surface
T_L	time required for the air at position L to reach the filter paper surface
V	volume of air sampled during period T
V_a	sample volume of particles of type s from above the filter
V_b	sample volume of particles of type s from below the filter
$V_{AC(s_2)}$	volume of air sampled during period $T_{AC(s_2)}$
V_L	volume of air sampled during period T_L
V_R	R-component of air velocity in air flow created by the filter holder
V_s	settling velocity of a particle of parameter s
V_Z	Z-component of air velocity in air flow
Z	particle coordinate along Z-axis
Z_c	position along Z-axis where $V_Z(Z, 0) = \lvert V_s \rvert$
Z_i	initial particle coordinate along Z-axis
Z_o	initial coordinate value along Z-axis
μ	air viscosity
ψ	current line function
ρ_p	particle density

1.0 INTRODUCTION

Aerosol sampling has been the object of much investigation. The purpose of aerosol sampling is to determine the concentration and the mass or size distribution of particles suspended in a given volume of air at a given time. A fundamental parameter required by the researcher is the sampling efficiency, defined as the fraction of particles of a given size and density that will be collected by a sampling system.

The sampling efficiency changes from one sampling system configuration to another. Calculations usually deal with the sampler orientation and air flow rate. Non-isokinetic conditions as studied by W.M. ter Kuile (Ref. 1) are discussed in his paper entitled "Comparable Dust Sampling at the Workplace (a contribution to the standardization of "total dust" measurements)". He draws the conclusion that the downward inlet arrangement best meets the requirements for standardization. His conclusion was based on the work of Walton (Ref. 2), Levin (Ref. 3), and Davies (Ref. 4) who developed theoretical models based on a point-source sink with a thin-walled filter holder. Parameters such as the sampling period and the height of the aerosol above the filter were not considered.

The present work involves a computer simulation of the interaction of particles undergoing sedimentation on a large-aperture inverted filter holder. Flow-field calculations are done by solving the Laplace equation for a flat disk with uniform air velocity over its surface. Critical distances are then obtained by iterative solution of the equations of motion. These distances are time-independent. The time-dependent sampling efficiency is obtained by combining critical distances and the sampler interaction distance for a given sample volume. Thus, the effect of various parameters such as the sampling flow rate, sampling period, height of the aerosol above the filter, and rim size can be evaluated. The sampling setup is illustrated in Fig. 1.

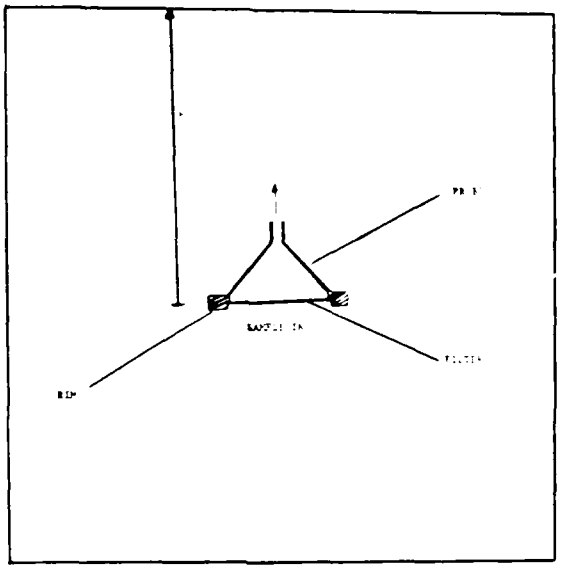

FIGURE 1 - Large entrance aperture sampler facing downward

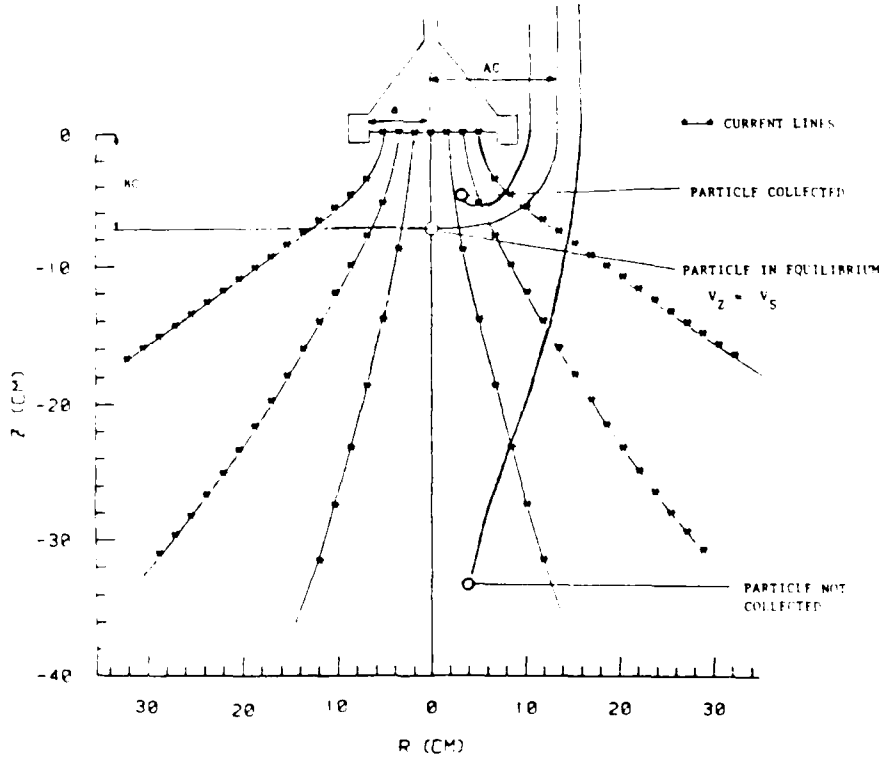

FIGURE 2 - Particles in air flow created by an inverted sampler

This work was conducted at DREV between February and December 1983 under PCN 21B05, Aerosols.

2.0 DETERMINATION OF CRITICAL POSITIONS

The critical position of a particle of radius r and density ρ_p is the closest position to the sampler at which the particle will not be collected by the sampler and thus will escape it. As long as the settling velocity of a particle (V_s) is lower than the airspeed on the filter paper of an inverted sampler, critical positions will exist.

In order to calculate critical positions, the equations of motion of a particle in a flow field created by an inverted filter holder have to be solved.

Figure 2 illustrates the interaction of particles with the flow field created by the inverted filter holder, the radius of which is a = 6.7 cm. Particle trajectories as indicated are only examples but the current lines shown are those created by a flat disk with uniform air velocity at its surface. It has been assumed that settling particles start interacting with the field only for $Z < 0$. The middle trajectory defines two critical positions: at $Z = 0$, $R = AC$ and at $Z = BC$, $R = 0$.

2.1 Equations of Motion of a Particle in a Flow Field Created by a Large Inverted Filter Holder

The equations of motion of a particle in a flow field created by a large inverted filter holder (taking into account the gravitational field and air viscosity) are:

$$\frac{d^2Z}{dt^2} = \frac{9\mu}{2\rho_p r^2}\left(V_Z(Z,R) - \frac{dZ}{dt}\right) - g \qquad [1]$$

$$\frac{d^2R}{dt^2} = \frac{9\mu}{2\rho_p r^2}\left(V_R(Z,R) - \frac{dR}{dt}\right) \qquad [2]$$

where

g: 981 cm/s^2

r: particle radius (cm)

t: time (s)

R: particle coordinate along R-axis

Z: particle coordinate along Z-axis

V_Z: Z-component of air velocity in air flow created by the filter holder

V_R: R-component of air velocity in air flow created by the filter holder

μ: air viscosity

ρ_p: density of the particle.

Velocities V_Z and V_R are calculated using the following expressions:

$$V_Z(Z,R) = \frac{-1}{R}\frac{\partial\psi(Z,R)}{\partial R} \qquad [3]$$

$$V_R(Z,R) = \frac{1}{R}\frac{\partial\psi(Z,R)}{\partial Z} \qquad [4]$$

where

$$\psi(Z,R) = \frac{-Q}{\pi a}\int_0^\infty \frac{e^{kz}}{k} J_1(kR)\, J_1(ka)\, dk \qquad [5]$$

where $Z < 0$

Q : sampling flow rate (SFR) (cm^3/s)

a : radius of the circular aperture

$J_1(\ )$: Bessel function of order 1

k : variable in Fourier-Bessel space.

Refer to Appendix A for relevant details.

Prior to the solution of the equations of motion, it is essential that the velocities V_Z and V_R be calculated. In order to do so, the function ψ is calculated over the area of interest for m x n positions. Using the definition of the derivative for the calculation of velocities V_Z and V_R, two matrices of size (m-1) x (n-1) are defined. Then, when the numerical solution of the equations of motion are required, values of flow velocity are obtained by interpolation (see Appendix B for more details).

2.2 Numerical Solution of the Equations of Motion, and the Criterion for Collection

The equations of motion are numerically solved using the fourth-order Runge-Kutta technique. Initial conditions of the position and velocities are as follows:

$$R_i = a$$

$$Z_i = Z_o$$

$$\frac{dZ}{dt} = V_s \text{ and } \frac{dR}{dt} = 0 \text{ at } t = 0$$

where V_s is the settling velocity of the particle and is equal to

$$\frac{2}{9}\frac{\rho_p g r^2}{\mu}. \qquad [6]$$

The equations of motion are solved for a given particle size and density. However, we will refer to a more general quantity, s, defined as $\rho_p r^2$. Particles of equal s will act in the same way.

The criterion for collection is simple because of the azimuthal symmetry of the problem: a particle will be collected if, at any time, $\frac{dZ}{dt}$ becomes greater than zero. A particle will not be collected if at any time $Z < Z_c$ (Z is negative-valued) where Z_c is the position at which $V_Z(Z_c, 0) = |V_s|$. This is on the axis where the velocity is maximum in the Z-direction.

Once the status of a given particle is known (whether it will be collected or not), the initial value R_i is increased or decreased. Its status is redefined and so on until the difference between the initial position of a collected particle and of an uncollected particle is smaller than a predetermined accuracy ΔR ($\simeq$ 0.1 cm). This position is called the critical distance AS for a given Z_i and s. A particle with these initial conditions is brought to R = 0 and stays motionless in the air at a distance Z where $V_Z(Z, 0) = |V_s|$. The particle weight and the air stream drag force are then in equilibrium.

2.3 Representation of Critical Positions on the Z-R Plane

Critical positions were calculated for a range of values of the parameter s at different initial heights (Z_i) for the two sampling flow rates Q of 30 L/min and 50 L/min. Figure 3 shows critical positions for an s of 90 and 160 g $\mu m^2/cm^3$; the continuous curves are potential lines created by a disk of radius 6.7 cm with uniform velocity over its surface. Critical positions can be represented by a family of ellipses with principal axes AC and BC along the R and Z axes respectively. Figures 4 and 5 show critical positions of the principal axes AC (+) and BC (-) as a function of s for sampling flow rates of 30 and 50 L/min. The smaller the particles, the farther the critical

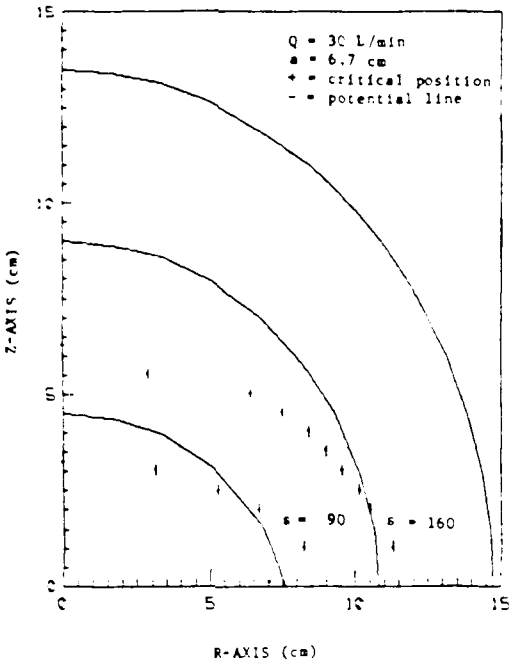

FIGURE 3 - Potential lines created by the sampler and critical positions for particles of parameter s of 90 and 160 g $\mu m^2/cm^3$

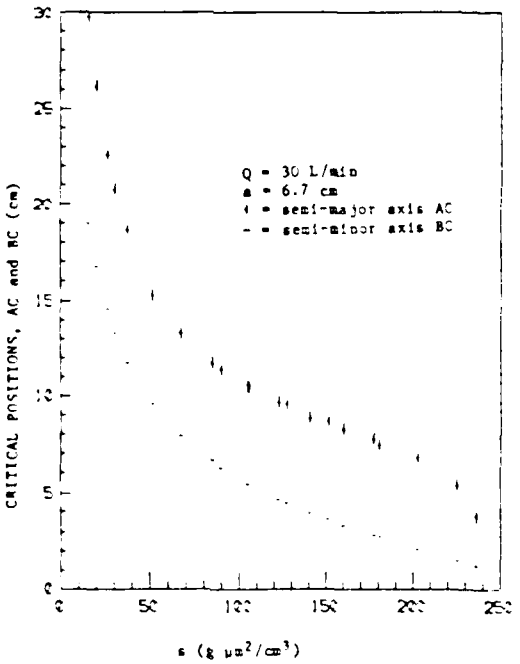

FIGURE 4 - Elliptical representation of critical position as a function of parameter s

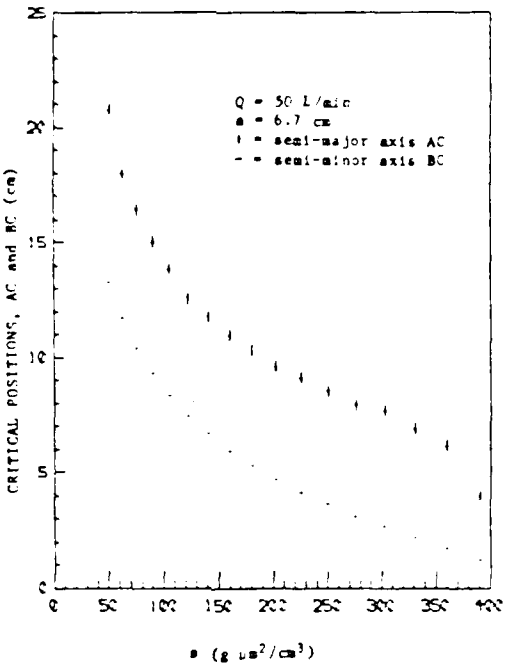

FIGURE 5 - Elliptical representation of critical position as a function of parameter s

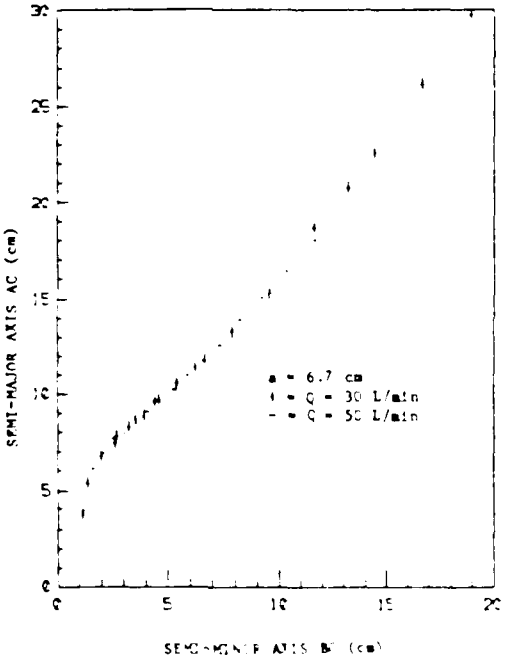

FIGURE 6 - R-axis elliptical representation of critical position (AC) as a function of Z-axis elliptical representation of critical position (BC)

position. AC is always greater than BC. Figure 6 shows critical position AC(s) as a function of BC(s). Sampling flow rate data for 30 L/min are represented by (+) while those obtained at 50 L/min are represented by (-). The two curves obtained agree fairly well with each other. For large values of BC(s), it appears that there is a linear relationship between the two principal critical position axes:

$$AC(s) \simeq 1.6\ BC(s) \qquad [7]$$

This expression may be used for extrapolation of critical positions for small s. Since BC(s) is easily calculated by finding the position on the Z-axis where $V_Z(Z, 0) = V_s$, critical positions can be obtained easily using [7].

3.0 TIME-DEPENDENCE OF SAMPLED VOLUME OF AEROSOL

Critical positions have been established for time-independent sampling. The volume of air QT (Q: sampling flow rate, T: sampling period) drawn through the filter defines the space where the air has been taken from. This space is bounded by a potential line which crosses the Z and R axes at positions B and A. As for critical positions, a good representation of the potential line could be given by a family of ellipses. A and B become halves of the principal axes of an ellipse. Figure 7 shows A and B versus sampled volume. The volume has been obtained by the evaluation of the integral for the rotation of the potential line around the Z-axis. So, for example, for a sampling flow rate of Q = 30 L/min and a sampling period of T = 1 min, a volume of 3.0×10^4 cm^3 of air is sampled. The rotated potential line (surface) that bounds this volume is half an ellipsoid of revolution with half-axis A and B equal to 24 and 25 cm.

Particles collected by the inverted sampler come from two areas: particles below the plane Z = 0 at t = 0, and those above the plane Z = 0 at t = 0. For particles below the plane Z = 0, the volume

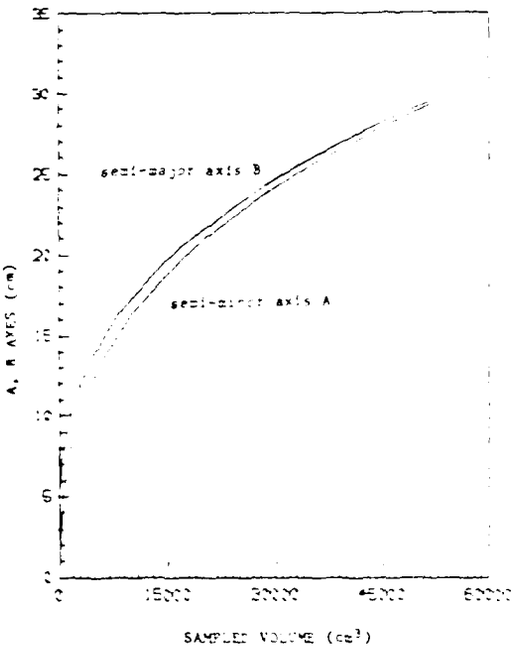

FIGURE 7 - Elliptical representation of sampled volume. The volumes delimited by potential lines created by the sampler are represented by ellipses of revolution around Z-axis

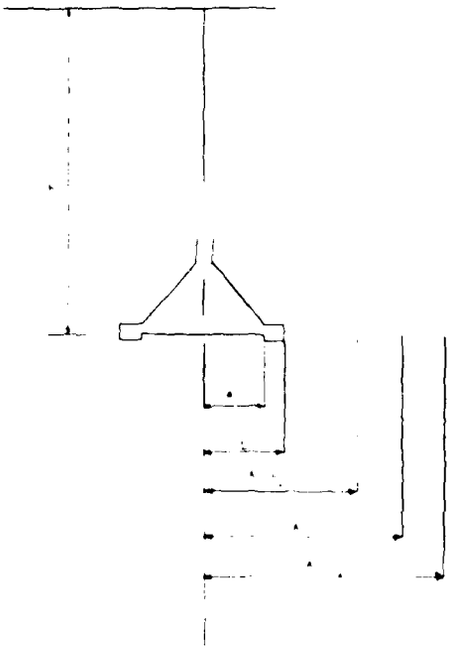

FIGURE 8 - Sampled volume of air and critical positions

bounded by critical positions and its interaction with the sampled volume are considered. For particles above the plane Z = 0, the height of the aerosol above the plane, the surface delimited by the critical distance at Z = 0, i.e. AC, and the interaction distance A of the sampler are considered.

3.1 Sampled Volume of Aerosol, Particle Below the Filter at t = 0

A sampled volume QT defines a volume delimited by a rotated potential line. This potential line and critical positions can be represented by ellipses with axes A, B, AC(s) and BC(s).

Three different cases have to be considered (see Fig. 8).

Case #1: The volume delimited by critical positions of a particle of given s is completely inside the sampled volume of air. The sampled volume of particles of type s $V_b(s,t)$ equals the volume delimited by the critical positions.

Case #2: The volume delimited by critical positions for a given s is completely outside the sampled volume of air. The sampled volume $V_b(s,t)$ of particles of type s equals the sampled volume of air.

Case #3: The volume delimited by critical positions for a given s is partially outside the sampled volume of air. The sampled volume of particles of type s $V_b(s,t)$ equals the volume of the shaded area.

The procedure used to calculate the sampled volume of an aerosol of type s is as follows:

a) polynomial representation of sampled volume of air; principal axes A and B as functions of QT;

b) polynominal representation of critical positions; principal axes AC and BC as functions of s;

c) identification as case 1, 2 or 3;

d) evaluation of sampled volume.

3.2 Sampled Volume of Aerosol, Particle Above the Filter at t = 0

A particle undergoing sedimentation will interact with the sampled air when it crosses the plane Z = 0. The sampled volume of particles $V_a(s,T)$ is equal to $H(s,T) \times S(s,T)$. These two functions represent the height of the aerosol and the equivalent surface crossed by a particle of type s for a sampling period T. Figure 9 shows the various parameters that have to be considered for the evaluation of these functions. The parameter h is the height of the aerosol above the sampler, the parameter a is the radius of the aperture (a = 6.7 cm), L is the radius of the sampler, A is the major axis of the ellipse delimiting the sampled volume, of air, and $AC(s_1)$ and $AC(s_2)$ are the axes delimiting these critical distances for particles of type s_1 and s_2.

3.2.1 Evaluation of S(s,T)

The function S(s,T) is defined by:

$$S(s,T) = \pi(\overline{AC}(s,T) - L^2) \text{ for } \overline{AC} > L$$

$$= 0 \qquad \text{for } \overline{AC} < L \qquad [8]$$

where $\overline{AC}(s,T)$ is the mean interactive distance during the sampling

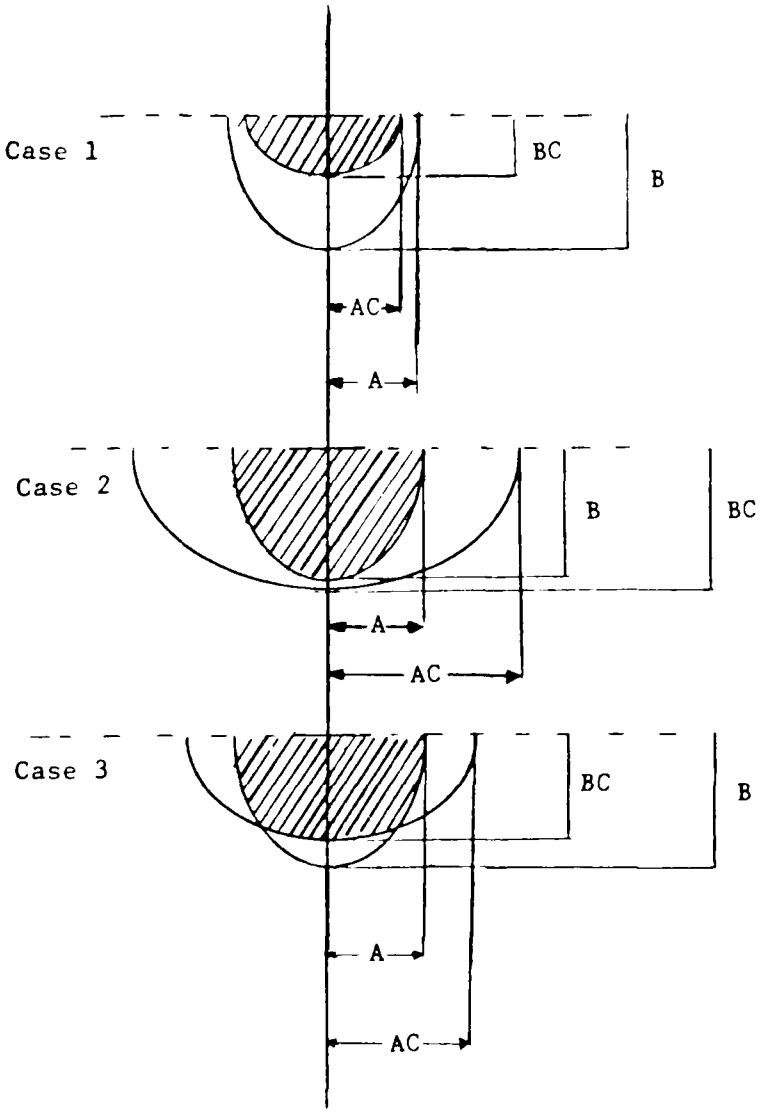

FIGURE 9 - Definition of parameters

period T. Particles of type S_1 and S_2 represent the two cases possible.

Case #1, $AC(s) > A$

Using the mean value theorem:

$$\overline{AC}(s,T) = \frac{1}{T - T_L} \int_{T_L}^{T} A(t)dt \qquad [9]$$

where A(t) is a function which represents the diminution of A as sampling proceeds, T_L is the time required for the air at position L to reach the filter paper surface.

Case #2, $AC(s) < A$

$$\overline{AC}(s,T) = \left(1 - \frac{T_{AC(s_2)}}{T}\right) AC(s_2) + \left(\frac{1}{T_{AC(s_2)} - T_L}\right) \int_{T_L}^{T_{AC(s_2)}} A(t)\, dt \qquad [10]$$

where $T_{AC(s_2)}$ is the time taken by the air at position $AC(s_2)$ to reach the filter paper surface.

Using the expressions $V = QT$, $V_L = QT_L$ and $V_{AC(s_2)} = QT_{AC(s_2)}$, the equations for cases 1 and 2 become:

$AC(s) > A$

$$\overline{AC(s,T)} = \frac{1}{V - V_L} \int_{V_L}^{V} A(V)dV \qquad [11]$$

$AC(s) < A$

$$\overline{AC(s,T)} = (1 - \frac{V_{AC(s_2)}}{V}) \cdot AC(s_2) + (\frac{1}{V_{AC(s_2)} - V_L}) \int_{V_L}^{V_{AC(s_2)}} A(V)dV \qquad [12]$$

Figure 6 shows the relation between A and V. A polynomial representation of A versus V is produced and then the integration can be easily performed.

3.2.2 Evaluation of H(s,T)

The function H(s,T) represents the height of the aerosol which crosses the interactive surface as a function of the parameter s, the height h of the aerosol above the filter, and the sampling period T.

The expression for the settling velocity and the speed given by the ratio h/T defines a particle of parameter s_c such that all particles with s greater than s_c cross the interactive surface in a period of time shorter than the sampling period T. For particles with s smaller than s_c, only a fraction at height h cross the interactive surface. This fraction is equal to the ratio of settling velocities or s/s_c. However, in both cases the height of the aerosol crossing the interactive surface has to be multiplied by the fraction of the sampled volume: $(1 - \frac{V_L}{V})$.

The function H(s,T) is:

$$H(s,T) = (1 - \frac{V_L}{V}) \cdot h \qquad \text{for } s > s_c \qquad [13]$$

$$= (1 - \frac{V_L}{V}) \cdot h \cdot \frac{s}{s_c} \qquad \text{for } s < s_c \qquad [14]$$

where

$$s_c = 9\mu h/2gT \qquad [15]$$

The procedure used to calculate the sampled volume of aerosol of type s is as follows:

a) polynomial representation of V as a function of A in order to determine V, V_L and $V_{AC(s_c)}$;

b) polynomial representation of A as a function of V in order to perform the integration;

c) identification of cases;

d) determination of s_c;

e) evaluation of sampled volume.

3.3 Estimation of Inertial Effects

In the previous sections, the interactive time of a particle with the air stream was not considered. It was assumed that a particle inside the interaction zone as defined previously was automatically collected. But it is now known that a particle at its critical position will never be collected. Hence, how far from its critical position does a particle have to be in order to be collected during the sampling period? In order to answer this question, the time taken by particles of s equal to 16, 100 and 200 g $\mu m^2/cm^3$ as a function of initial position R = 0 and Z = X BC(s) with X[0.1 - 0.99], and BC(s), the critical position on the Z-axis has been calculated using [1], [2], [3] and [4].

Figure 10 shows the results of these calculations. The vertical lines represent critical positions. Also shown on the graph is the time taken by the air at a position Z and R = 0 to cross the filter plane (Z = 0). These curves were obtained for a sampling flow rate of 50 L/min. For a 60-s sampling period it appears that for s greater than 100, a particle at 0.99 BC will be collected in less than 20 s. However, for s = 16, particles at a position above 0.94 BC will not be collected. In order to attain 0.99 BC for s = 16, the sampling period would have to be extended to 150 s. It can be seen that the inertial effects are not very important. However it is important to remember that neglecting them will result in an overestimation of the volume sampled, especially for small particles.

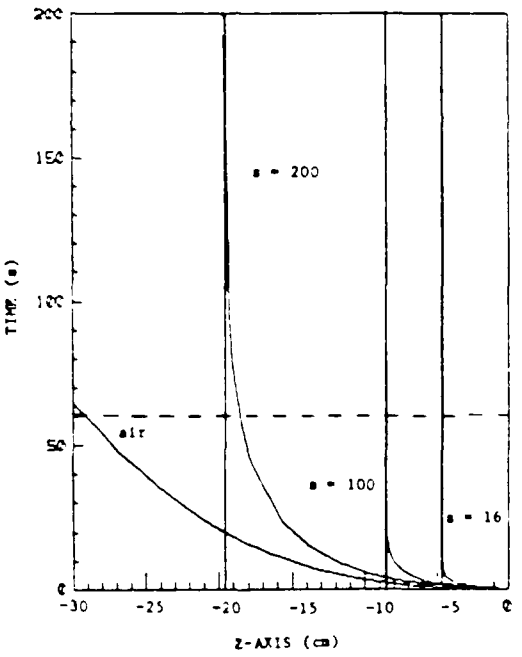

FIGURE 10 - Capture time as a function of distance along Z-axis for three values of S

4.0 SAMPLING EFFICIENCY

The sampling efficiency E is defined as the ratio of the sampled volume of particles ($V_b(\ ) + V_a(\ )$) of parameter value s to the sampled volume of air QT:

$$E(s) = \frac{V_b(\ ) + V_a(\ )}{QT} \qquad [16]$$

Figures 11 and 12 show the contribution to the total efficiency (+++) of particles above (——) and below (---) the plane Z = 0 at sampling flow rates of 50 and 30 L/min. Other parameters were h = 100 cm, T = 60 s and rim size = 2.3 cm. It is clearly shown that for small s, the main contribution to the total efficiency comes from below the plane Z = 0. As s tends toward zero, the contribution from below the plane Z = 0 tends toward unity; the contribution from above the plane tends toward zero. The contribution to E for particles under the plane is zero for s with $\overline{AC} < L$.

Figures 13 to 17 show the influence of height (h), sampling period (T), sampling flow rate (Q) and rim size (L - a).

The sampling flow rate effect on sampling efficiency is shown for the two flow rates of 30 and 50 L/min in Fig. 13. Other parameter values are T = 60 s, h = 100 cm and rim size = 2.3 cm. As expected, the sampling efficiency increases with increasing sampling flow rate.

Figure 14 shows the height dependence of sampling efficiency for h = 0, 50 and 100 cm. Other parameter values were Q = 30 L/min, rim size = 2.3 cm and T = 60 s. The difference in E is quite large between h = 0 cm and the other two heights. The difference is however quite small between h = 50 and 100 cm. There, s_c was determined by [15] as 66.5 and 133.8 g $\mu m^2/cm^3$ respectively. This is why the difference appears for values of s greater than 66.5 g $\mu m^2/cm^3$. For values of s greater than 135 g $\mu m^2/cm^3$, the volume collected comes only from

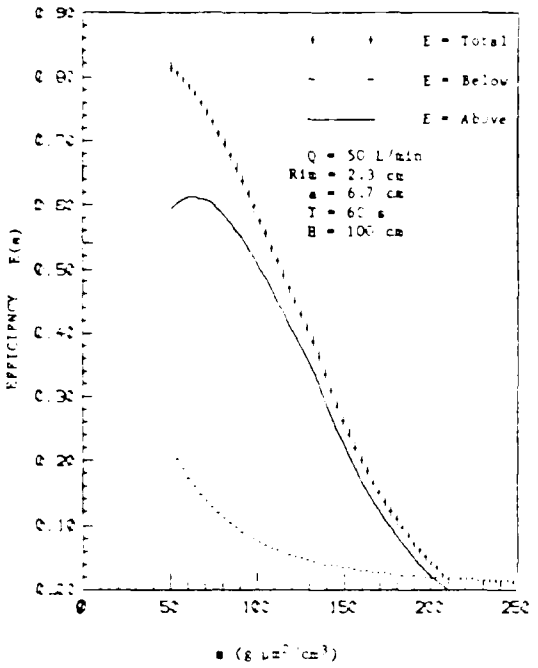

FIGURE 11 - Sampler efficiency in collecting particles from above and below the orifice

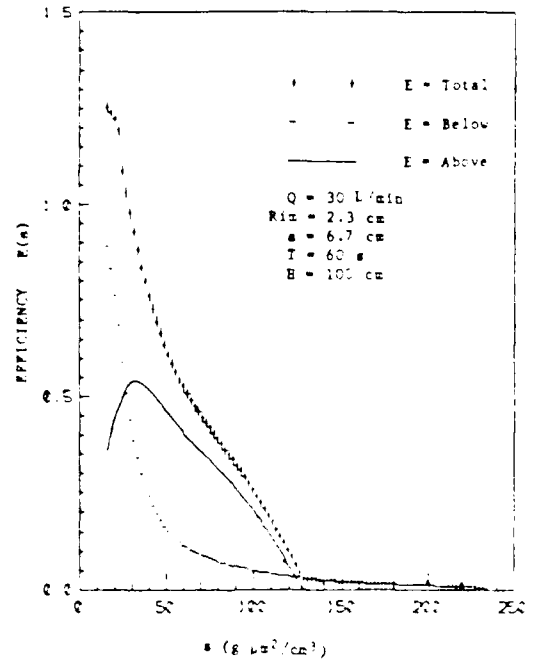

FIGURE 12 - Sampler efficiency in collecting particles from above and below the orifice

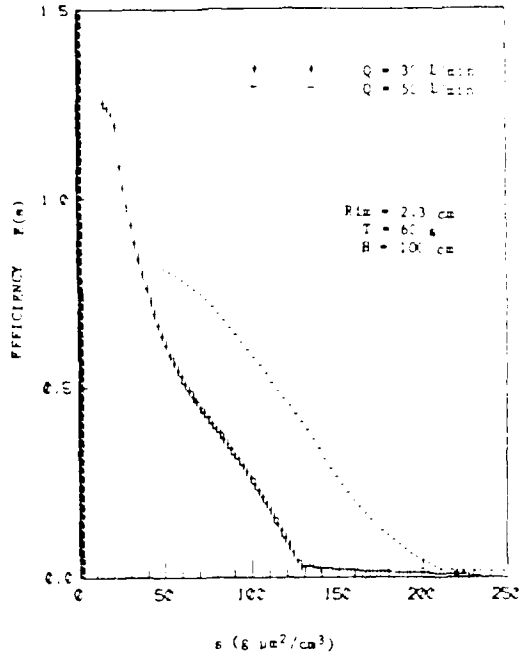

FIGURE 13 - Influence of sampling flow rate on sampling efficiency

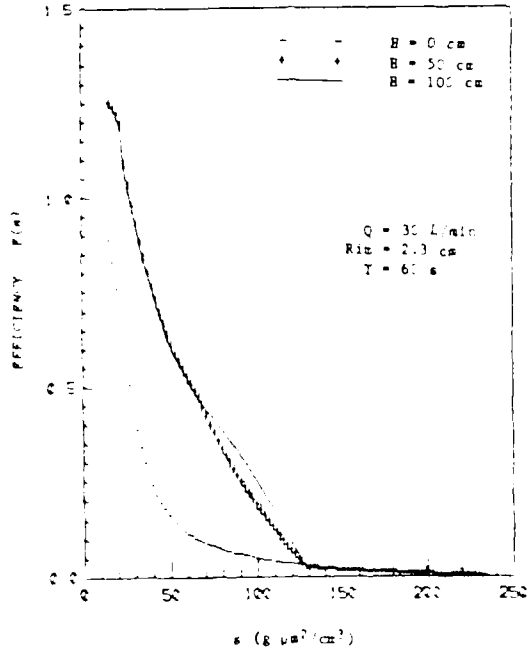

FIGURE 14 - Influence of sampling height on sampling efficiency

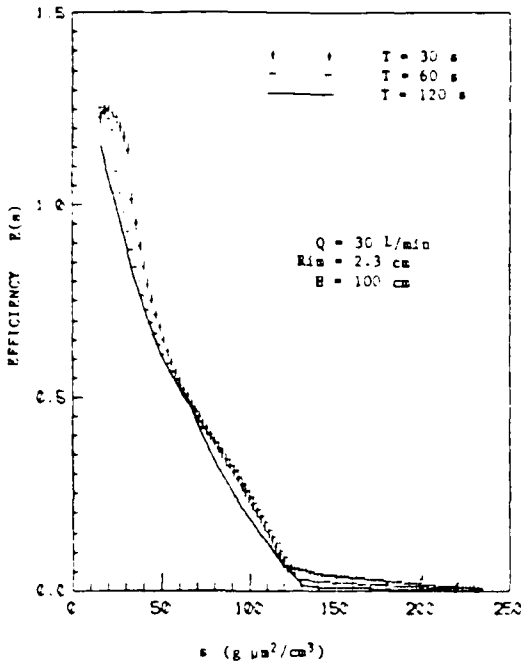

FIGURE 15 - Influence of sampling period on sampling efficiency

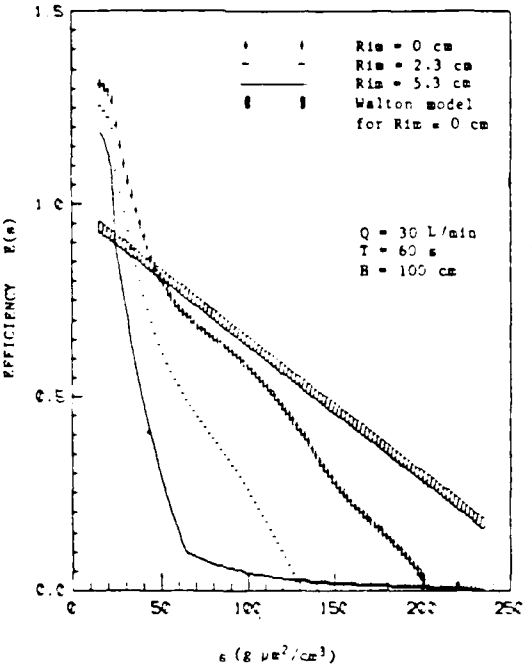

FIGURE 16 - Influence of sampler rim size on sampling efficiency

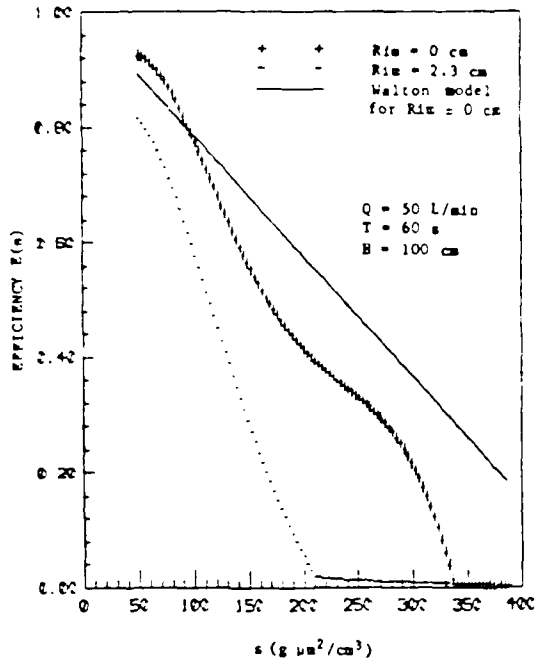

FIGURE 17 - Influence of sampler rim size on sampling efficiency

below the filter. This is because critical positions AC(s) for $s > 135$ g $\mu m^2/cm^3$ are below 9 cm, which is the radius (L) of the sampler (6.7 + 2.3 cm).

The sampling period (T) dependence is shown for three sampling periods (30, 60 and 120 s) in Fig. 15. Other parameter values were Q = 30 L/min, h = 100 cm, rim size = 2.3 cm. The s_c are 267, 133.8 and 66.8 g $\mu m^2/cm^3$ respectively. There is no significant difference between these three curves. As with the height dependence curves, these curves cross one another at s_c = 66 g $\mu m^2/cm^3$. The contribution of particles below the filter becomes less important as T increases.

The effect of rim size on sampling efficiency is shown in Figs. 16 and 17. Parameter values were h = 100 cm, T = 60 s, rim

sizes = 0, 2.3, 5.3 cm. In Fig. 16, Q = 30 L/min and in Fig. 17, 50 L/min. The larger the rim, the lower the contribution from above the filter. For the limiting case of a rim size larger than A (which is where the potential line delimiting the sampled volume crosses the sampler active surface plane), only particles below the filter will contribute to the efficiency. As the rim gets smaller, the contribution of particles above the filter to total efficiency becomes more and more important. However, for particles with large s ($s > 200$ g $\mu m^2/cm^3$, Fig. 16; $s > 340$ g $\mu m^2/cm^3$, Fig. 17), only particles directly below the filter will be collected. This is not due to a short sampling period but rather to the relatively low speed of air for regions not directly in front of the filter. Also shown in Figs. 16 and 17 are the curves of sampling efficiency as predicted by Walton (Ref. 2), which states that for a very thin rim, efficiency is given by the expression

$$1 - \frac{V_s}{V} \qquad [17]$$

where

V_s: settling velocity of particles

V: airspeed at the filter.

This theory does not take into account the height of the aerosol above the sampler and the sampling period, and it assumes a very small rim size.

5.0 CONCLUSIONS

A computer simulation has been used to calculate the sampling efficiency of an inverted sampler with a large entrance aperture. It has been shown that the sampling efficiency can be represented by the

sum of the sampling efficiencies of particles above and below the sampler. As particle sizes tend towards zero, the main contribution to total efficiency comes from particles below the sampler. For very small particles, the sampling efficiency tends toward unity.

The height and the sampling period of aerosols above the sampler have a strong influence on sampling efficiency. The sampling efficiency of large particles increases with height and sampling period. However, the sampling efficiency is height-independent for heights greater than $\frac{2g\rho r_a^2 T}{9\mu}$, where r_a is the cut-off particle size collected for particles above the sampler plane. Note the linear relationship between the height and the sampling period T. As expected, a higher sampling flow rate allows collection of larger particles. Finally, a smaller rim size will provide a higher sampling efficiency, especially for large particles.

The approach is general enough to be applied to other inverted samplers. An improvement to this simulation would be the use of the exact flow-field calculations around the sampler.

6.0 REFERENCES

1. Kuile, W.M. ter, "Comparable Dust Sampling at the Workplace", IMG-TNO Report F1699, Instituut voor milieuhygiene en gezondheidstechniek, Delft, The Netherlands, September 1979, UNCLASSIFIED

2. Walton, W.H., "Theory of Size Classification of Airborne Dust Clouds by Elutriation", Brit. J. Appl. Phys., Vol. 5, Suppl. No. 3, p. 529, 1954.

3. Levin, L.M., "Investigations in the Physics of Coare-dispersed Aerosols", Izv, Akad. Nauk SSSR; Translated: Foreign Tech. Div. Ohio, 1961.

4. Davies, C.N., "The Entry of Aerosols into Sampling Tubes and Heads", Brit. J. Appl. Phys. (J. Phys. D), Vol. 1, pp. 929-932, May 1968.

APPENDIX A

Potential and Flow Lines Created by a Flat Disk with Uniform Velocity across its Surface

The Laplace equation in cylindrical coordinates is:

$$\frac{\partial^2\Phi}{\partial Z^2} + \frac{\partial^2\Phi}{\partial R^2} + \frac{1}{R}\frac{\partial\Phi}{\partial R} + \frac{1}{R^2}\frac{\partial^2\Phi}{\partial\Theta^2} \qquad [A-1]$$

In the case of symmetry about the Z-axis, there is no Θ-dependence. A particular solution is then $\Phi = e^{kz}J_o(kR)$ for $z < 0$ where k is a positive integration constant in the Fourier-Bessel space.

Using Fourier-Bessel expansion and the boundary condition that on the surface ($z = 0$), $-\frac{\partial\Phi}{\partial Z} = f(R)$, a general solution is obtained (Ref. A1), i.e.:

$$\Phi = \int_o^\infty e^{kz}\, J_o(kR)dR \int_o^\infty f(R')\, J_o(kR')\, R'\, dR' \qquad [A-2]$$

If the speed is uniform over the disk of radius $R = a$ at $z = 0$, and since

$$\int_o^\infty J_o(kR')\, R'\, dR' = \frac{a}{k}\, J_1\,(ka) \qquad [A-3]$$

the solution becomes

$$\Phi = aV \int_o^\infty e^{kz}\, J_o(kR)\, J_1(ka)\, \frac{dk}{k} \qquad [A-4]$$

The expression for the current lines is obtained using the theorem of nul divergence for a harmonic function, i.e.:

$$\vec{\nabla} \cdot \vec{V} = \frac{1}{R}\frac{\partial}{\partial R}(\rho V_R) + \frac{\partial}{\partial Z} V_Z = 0 \qquad [A-5]$$

then

$$V_R = -\frac{1}{R}\frac{\partial \psi}{\partial Z} \text{ and } V_Z = \frac{1}{R}\frac{\partial \psi}{\partial R} \qquad [A-6]$$

and furthermore:

$$\nabla\phi = \frac{\partial \phi}{\partial R}\hat{e}_R + \frac{\partial \phi}{\partial Z}\hat{e}_Z$$

$$= V_R \hat{e}_R + V_Z \hat{e}_Z \qquad [A-7]$$

Then, using [A-5] and [A-6], we obtain

$$-\frac{1}{R}\frac{\partial \psi}{\partial Z} = \frac{\partial \phi}{\partial R} \; ; \; \frac{1}{R}\frac{\partial \psi}{\partial R} = \frac{\partial \phi}{\partial Z}$$

Integrating,

$$\psi = -R\int \frac{\partial \phi}{\partial R}\, dZ; \text{ or } \psi = \int \frac{\partial \phi}{\partial Z}\, RdR \qquad [A-8]$$

using equations [A-7] and [A-4], [A-4] becomes

$$\psi = -aV\int_0^\infty \frac{e^{kZ}}{k} J_1(kR)\, J_1(ka)\, dK \qquad [A-9]$$

Using the expression relating the sampling flow rate Q to the area of the disk, $V = \frac{Q}{\pi a^2}$, the product aV can be replaced by $\frac{Q}{\pi a}$.

REFERENCE

A1. Lamb, H., "Hydrodynamics", Dover Publications, New York, 1932.

APPENDIX B

Note on Velocity Calculation

Equation A-8 has been used to calculate current lines in the space R-Z. A matrix of m x n elements represents this region of space (m = n = 21). Velocities V_R and V_Z are calculated using the following expressions:

$$V_R = -\frac{1}{R}\frac{\partial\psi}{\partial Z} \longrightarrow V_{RN}(I,J) = \frac{1}{(J-1)\Delta R} \cdot \frac{\psi(I+1,J) - \psi(I,J)}{\Delta Z} \qquad [B-1]$$

$$V_Z = \frac{1}{R}\frac{\partial\psi}{\partial R} \longrightarrow V_{ZN}(I,J) = \frac{1}{\frac{1}{2}(2J-1)\Delta R} \cdot \frac{\psi(I,J+1) - \psi(I,J)}{\Delta R} \qquad [B-2]$$

where ΔZ and ΔR are distances between nodes on the R and Z axes; $V_{RN}(I,J)$ and $V_{ZN}(I,J)$ are velocities on nodes along the R and Z axes. ΔZ and ΔR have been set to 1.5 and 1.68 cm, which is a/4.

The position of nodes for the velocities matrix is summarized in Table B-I.

TABLE B-I

	Node on R-axis	Node on Z-axis
V_{RN}	$(J-1)\Delta R$	$\frac{1}{2}(2I-1)\Delta Z$
V_{RN}	$\frac{1}{2}(2J-1)\Delta R$	$(I-1)\Delta Z$

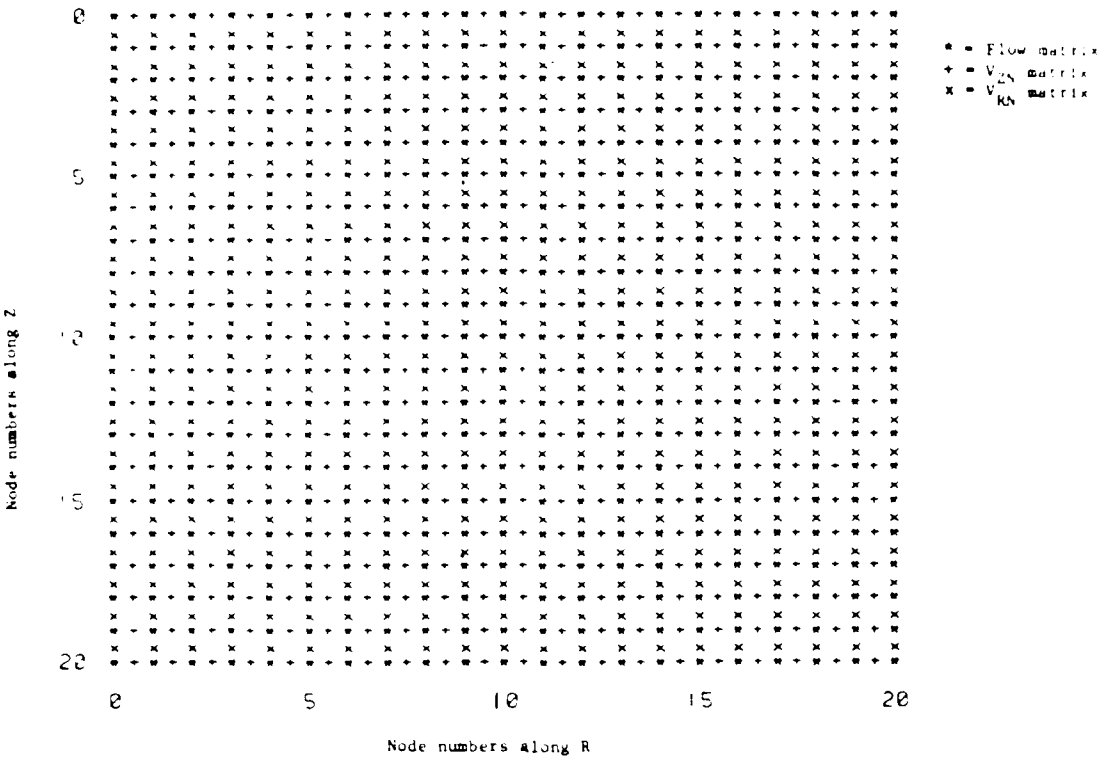

FIGURE B1 - Position of nodes for ψ, V_{RN} and V_{ZN}

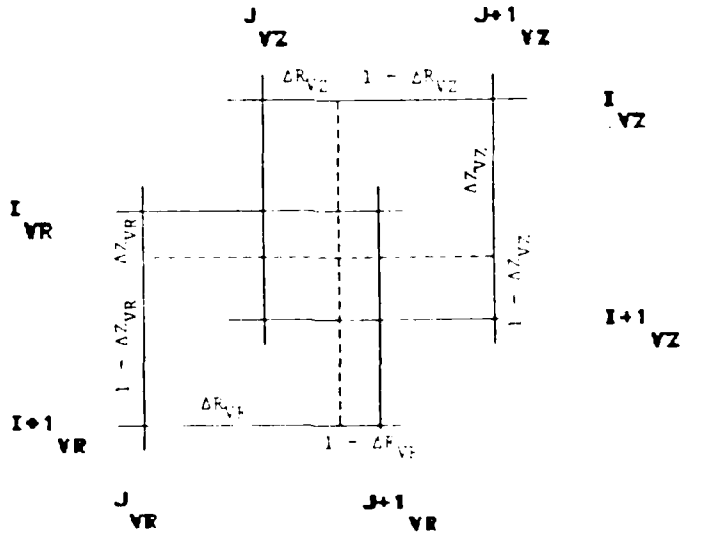

FIGURE B2 - Definition of variables for the calculation of internodal velocities

The velocity matrix has (m - 1) x (n - 1) elements and they are not superimposed one on another. Figure B1 shows the position of nodes for ψ with (*), V_{RN} with (X) and V_{ZN} with (+).

Internodal velocities are calculated using interpolation equations (see Fig. B2).

$$V_R = (1-\Delta Z_{VR})\,((1-\Delta R_{VR})\,V_{RN}(I,J) + \Delta R_{VR} V_{RN}\,(I+1,J))$$

$$+ \Delta Z_{VR}((1-\Delta R_{VR})V_{RN}(I+1,J) + \Delta R_{VR} V_{RN}(I+1,J+1))$$

[B-3]

$$V_Z = (1-\Delta R_{VZ})\,((1-\Delta Z_{VZ})\,V_{ZN}(I,J) + \Delta Z_{VZ}\,V_{ZN}(I+1,J))$$

$$+ \Delta R_{VZ}\,((1-\Delta Z_{VZ})\,V_Z(I,J+1) + \Delta Z_{VZ}\,V_{ZN}(I+1,J+1))$$

[B-4]

where internodal distances ΔR and ΔZ have been normalized to 1.

DREV R-4399/86 (UNCLASSIFIED)

Research and Development Branch, DND, Canada.
DREV, P.O. Box 8800, Courcelette, Que. G0A 1R0

"On the Sampling Efficiency of a Large Downward Inlet Aerosol Sampler"
by G. Roy

A computer simulation has been used to calculate the sampling efficiency of a downward-facing aerosol sampler having a large entrance aperture. Flow-field calculations have been done by solving the Laplace equation for a flat disk with uniform air velocity over its surface. Initial positions from which particles reach an equilibrium position at which the sedimentation speed equals the air suction speed of the sampler are obtained by iterative solution of the equations of motion. These distances are time-independent and are called critical distances. The time-dependent sampling efficiency is obtained by combining critical distances with the sampler interaction distance for a given sample volume of air. The effect on sampling efficiency of various parameters such as the sampling flow rate, sampling period, height of the aerosol above the filter, and rim size is evaluated.

DREV R-4399/86 (UNCLASSIFIED)

Research and Development Branch, DND, Canada.
DREV, P.O. Box 8800, Courcelette, Que. G0A 1R0

"On the Sampling Efficiency of a Large Downward Inlet Aerosol Sampler"
by G. Roy

A computer simulation has been used to calculate the sampling efficiency of a downward-facing aerosol sampler having a large entrance aperture. Flow-field calculations have been done by solving the Laplace equation for a flat disk with uniform air velocity over its surface. Initial positions from which particles reach an equilibrium position at which the sedimentation speed equals the air suction speed of the sampler are obtained by iterative solution of the equations of motion. These distances are time-independent and are called critical distances. The time-dependent sampling efficiency is obtained by combining critical distances with the sampler interaction distance for a given sample volume of air. The effect on sampling efficiency of various parameters such as the sampling flow rate, sampling period, height of the aerosol above the filter, and rim size is evaluated.

DREV R-4399/86 (UNCLASSIFIED)

Research and Development Branch, DND, Canada.
DREV, P.O. Box 8800, Courcelette, Que. G0A 1R0

"On the Sampling Efficiency of a Large Downward Inlet Aerosol Sampler"
by G. Roy

A computer simulation has been used to calculate the sampling efficiency of a downward-facing aerosol sampler having a large entrance aperture. Flow-field calculations have been done by solving the Laplace equation for a flat disk with uniform air velocity over its surface. Initial positions from which particles reach an equilibrium position at which the sedimentation speed equals the air suction speed of the sampler are obtained by iterative solution of the equations of motion. These distances are time-independent and are called critical distances. The time-dependent sampling efficiency is obtained by combining critical distances with the sampler interaction distance for a given sample volume of air. The effect on sampling efficiency of various parameters such as the sampling flow rate, sampling period, height of the aerosol above the filter, and rim size is evaluated.

DREV R-4399/86 (UNCLASSIFIED)

Research and Development Branch, DND, Canada.
DREV, P.O. Box 8800, Courcelette, Que. G0A 1R0

"On the Sampling Efficiency of a Large Downward Inlet Aerosol Sampler"
by G. Roy

A computer simulation has been used to calculate the sampling efficiency of a downward-facing aerosol sampler having a large entrance aperture. Flow-field calculations have been done by solving the Laplace equation for a flat disk with uniform air velocity over its surface. Initial positions from which particles reach an equilibrium position at which the sedimentation speed equals the air suction speed of the sampler are obtained by iterative solution of the equations of motion. These distances are time-independent and are called critical distances. The time-dependent sampling efficiency is obtained by combining critical distances with the sampler interaction distance for a given sample volume of air. The effect on sampling efficiency of various parameters such as the sampling flow rate, sampling period, height of the aerosol above the filter, and rim size is evaluated.

CRDV R-4399/86 (SANS CLASSIFICATION)

Bureau - Recherche et Développement, MDN, Canada.
CRDV, C.P. 8800, Courcelette, Qué. G0A 1R0

"L'efficacité de collection d'un échantillonneur d'aérosol à grande ouverture orienté vers le bas" par G. Roy

Une simulation sur ordinateur a été utilisée pour calculer l'efficacité d'un échantillonneur d'aérosol inversé à grande ouverture. Les champs d'écoulement ont été calculés en solutionnant l'équation de Laplace pour un disque plat dont la vitesse de l'air est uniforme sur la surface. Les positions initiales desquelles les particules aboutissent en équilibre à une position où la vitesse de sédimentation égale la vitesse de succion de l'air de l'échantillonneur sont établies par itération des équations du mouvement. Ces distances, appelées distances critiques, sont indépendantes du temps. La dépendance temporelle de l'efficacité d'échantillonnage est obtenue en combinant les distances critiques et la distance d'interaction pour un certain volume d'air. L'influence sur l'efficacité d'échantillonnage des paramètres tels que le débit et la période d'échantillonnage, la hauteur d'aérosol au-dessus de l'échantillonneur et la largeur du rebord est calculée.

CRDV R-4399/86 (SANS CLASSIFICATION)

Bureau - Recherche et Développement, MDN, Canada.
CRDV, C.P. 8800, Courcelette, Qué. G0A 1R0

"L'efficacité de collection d'un échantillonneur d'aérosol à grande ouverture orienté vers le bas" par G. Roy

Une simulation sur ordinateur a été utilisée pour calculer l'efficacité d'un échantillonneur d'aérosol inversé à grande ouverture. Les champs d'écoulement ont été calculés en solutionnant l'équation de Laplace pour un disque plat dont la vitesse de l'air est uniforme sur la surface. Les positions initiales desquelles les particules aboutissent en équilibre à une position où la vitesse de sédimentation égale la vitesse de succion de l'air de l'échantillonneur sont établies par itération des équations du mouvement. Ces distances, appelées distances critiques, sont indépendantes du temps. La dépendance temporelle de l'efficacité d'échantillonnage est obtenue en combinant les distances critiques et la distance d'interaction pour un certain volume d'air. L'influence sur l'efficacité d'échantillonnage des paramètres tels que le débit et la période d'échantillonnage, la hauteur d'aérosol au-dessus de l'échantillonneur et la largeur du rebord est calculée.

CRDV R-4399/86 (SANS CLASSIFICATION)

Bureau - Recherche et Développement, MDN, Canada.
CRDV, C.P. 8800, Courcelette, Qué. G0A 1R0

"L'efficacité de collection d'un échantillonneur d'aérosol à grande ouverture orienté vers le bas" par G. Roy

Une simulation sur ordinateur a été utilisée pour calculer l'efficacité d'un échantillonneur d'aérosol inversé à grande ouverture. Les champs d'écoulement ont été calculés en solutionnant l'équation de Laplace pour un disque plat dont la vitesse de l'air est uniforme sur la surface. Les positions initiales desquelles les particules aboutissent en équilibre à une position où la vitesse de sédimentation égale la vitesse de succion de l'air de l'échantillonneur sont établies par itération des équations du mouvement. Ces distances, appelées distances critiques, sont indépendantes du temps. La dépendance temporelle de l'efficacité d'échantillonnage est obtenue en combinant les distances critiques et la distance d'interaction pour un certain volume d'air. L'influence sur l'efficacité d'échantillonnage des paramètres tels que le débit et la période d'échantillonnage, la hauteur d'aérosol au-dessus de l'échantillonneur et la largeur du rebord est calculée.

CRDV R-4399/86 (SANS CLASSIFICATION)

Bureau - Recherche et Développement, MDN, Canada.
CRDV, C.P. 8800, Courcelette, Qué. G0A 1R0

"L'efficacité de collection d'un échantillonneur d'aérosol à grande ouverture orienté vers le bas" par G. Roy

Une simulation sur ordinateur a été utilisée pour calculer l'efficacité d'un échantillonneur d'aérosol inversé à grande ouverture. Les champs d'écoulement ont été calculés en solutionnant l'équation de Laplace pour un disque plat dont la vitesse de l'air est uniforme sur la surface. Les positions initiales desquelles les particules aboutissent en équilibre à une position où la vitesse de sédimentation égale la vitesse de succion de l'air de l'échantillonneur sont établies par itération des équations du mouvement. Ces distances, appelées distances critiques, sont indépendantes du temps. La dépendance temporelle de l'efficacité d'échantillonnage est obtenue en combinant les distances critiques et la distance d'interaction pour un certain volume d'air. L'influence sur l'efficacité d'échantillonnage des paramètres tels que le débit et la période d'échantillonnage, la hauteur d'aérosol au-dessus de l'échantillonneur et la largeur du rebord est calculée.

END

DTIC

8-86